LA-UR-80-2810

MASTER

TITLE: TWO-DIMENSIONAL RADIATION-HYDRODYNAMICS CALCULATIONS OF THE FORMATION OF O-B ASSOCIATION IN DENSE MOLECULAR CLOUDS

AUTHOR(S): Richard I. Klein, Univ. of Calif., Berkeley,
Maxwell T. Sandford, II, G-6, LASL and
Rodney W. Whitaker, G-6, LASL

SUBMITTED TO: Proceedings IAU Colloquium on Stellar Hydrodynamics

University of California

LOS ALAMOS SCIENTIFIC LABORATORY
Post Office Box 1663 Los Alamos, New Mexico 87545
An Affirmative Action/Equal Opportunity Employer

Form No. 836 R3
St. No. 2629
12/78

UNITED STATES
DEPARTMENT OF ENERGY
CONTRACT W-7405-ENG-36

Two-Dimensional Radiation-Hydrodynamics Calculations of the Formation of O-B Associations in Dense Molecular Clouds

Richard I. Klein*
Dept. of Astronomy, U. of Calif., Berkeley
Maxwell T. Sandford II and Rodney W. Whitaker
University of California, Los Alamos Scientific Laboratory

* Authors listed alphabetically

ABSTRACT

Two-dimensional calculations of ionization-shockwave propagation into a curved molecular cloud are presented. Density enhancement occurs due to the combined effects of cloud curvature and radiation flow. The star formation process is expected to be enhanced near the edges of irregularly shaped molecular clouds.

INTRODUCTION

O-B associations are groups of massive, young stars containing at least one O-type star and are 50-100 pc in linear extent. Blaauw (1964) found that stars in these associations were often separated as subgroups 10-40 pc apart and that the subgroups represent a temporal sequence with the oldest at one end of the association and the youngest at the other. Ambartsumian (1958) noted the occurrence of associations in dense interstellar clouds and Lynds (1980) discussed this relationship in connection with Elmegreen and Lada's (1977) sequential star formation model. This model describes the formation of O-B stars as a consequence of ionization and shock fronts (I-S) originating from the most recently formed O-stars in a subgroup. The ionization front at the edge of a molecular cloud is preceded by a strong shock. Radiative cooling in the isothermally compressed region keeps the dense cloud material at low ($\leq$100°K) temperature and the cooled, post-shock (CPS) layer eventually becomes gravitationally unstable, fragments, and produces the next stellar generation that repeats the process until the molecular cloud is exhausted. In addition, Hunter (1979) showed that Jeans' criterion is relaxed in the presence of a velocity field. Important questions are left unanswered by Elmegreen and Lada's semi-quantitative analysis. This paper addresses our initial effort to numerically solve the fully coupled equations of radiation-hydrodynamics in two space dimensions. These calculations follow the early stages of the I-S star formation process.

FORMULATION

We have developed a new numerical code for the solution of two-phase, radiative-transfer, Eulerian dynamics (TOP-RATED), which includes many of the physical processes necessary to study the interaction of O-star clusters with dense molecular clouds.

Hydrodynamics of two-phase (gas and dust) flow is calculated in cylindrical Eulerian coordinates using the partially implicit method given by Rivard and Torrey (1977). The non-grey equation of transfer is explicitly solved using the SN difference method of Lathrop and Brinkley (1973), which solves for the angular dependence of the specific monochromatic intensity and permits inclusion of anistopropic scattering. Additional equations solved explicitly are rate equations for H and He ionization and the Poisson equation for gravitational potential. Gravitational acceleration is negligible in the early stages and not is included in the present calculation

This paper presents results for a cloud of atomic hydrogen devoid of dust. More elaborate two-phase clouds will be considered in future work. The energy and rate equations solved in this paper for I, the specific internal energy including thermal and ionization contributions; and n_e, the electron number density are

$$\frac{\partial I}{\partial t} + \vec{V} \cdot \vec{V}\,(\rho I) = -\,p\,\vec{V}\cdot\vec{V} - \bar{\bar{\sigma}}\,(\vec{V}\,\vec{V}) - \vec{V}\cdot\kappa\,\vec{V}\,(T) - \lambda(T) n_{H_2}\,\theta +$$

$$n_{H^0}\int_{\nu_0}^{\infty} 4\pi J_\nu a_\nu\, d\nu - n_{H^+} n_e\,\alpha(T)\,(kT + h\nu_0) \quad , \quad \left(n_{H^+} = n_e\right) \tag{1}$$

and

$$\frac{\partial n_e}{\partial t} = n_{H^0}\int_{\nu_0}^{\infty} \frac{4\pi J_\nu}{h\nu}\, a_\nu\, d_\nu - n_e n_{H^+}\,\alpha(T) \quad , \tag{2}$$

where J_ν is the mean monochromatic intensity; α, the recombination coefficient; n_{H^0}, the number density of neutral hydrogen atoms; n_{H_2}, the number density of hydrogen molecules; κ, the electron heat conduction coefficient; $\bar{\bar{\sigma}}$, the viscous stress tensor; λ, the cooling rate for molecular hydrogen; and θ is a cut-off function: equal 1 if the relative fraction of hydrogen ions <1% and 0 otherwise. These equations are closed by relating mass density to the populations. Details of the full numerical treatment, including all equations solved will be given in a forthcoming paper. In this work, recombination radiation is not included in the source term of the transfer equation with consequence that temperature in the I-front is slightly under estimated. In this work we take the recombination cooling coefficient equal to the recombination rate coefficient.

INITIAL MODEL

This paper presents results for a 25 x 50 grid in r-z cylindrical coordinates, with $\Delta z = \Delta r = 1 \times 10^{15}$ cm. On all vector plots of results, the left ordinate represents the symmetry axis. For additional clarity, certain variables are plotted as surfaces over the r-z coordinate mesh, as in Fig. 1., which shows $\rho(r, z)$ used for initial conditions. This plot compresses the z coordinate by a factor of 2, and the symmetry axis is at the left, in the vertical direction. The incident ionizing radiation from the recently formed subgroup is represented by imposition of diffuse flux incident at the lower (radial) boundary. This flux is generated by geometric dilution of blackbody radiation at T = 30000°K to a value appropriate for an O9 star at 8 pc distance.

The initial cloud is neutral hydrogen at $n_H = 540/cm^3$ and T = 15°K, surrounded by ionized gas with $n_e = 0.34/cm^3$ and T = 15000°K at approximately pressure equilibrium. The optical thickness of a computing cell to ionizing radiation is approximately 0.5. The thickness of the I-front for 10 km/s velocity is $0.2/n_e$ pc (Spitzer, 1978), or approximately 2 cells in our calculation. The shock thickness (10^{11} cm) is below the resolution of the mesh and one therefore expects some structure to be resolved in the I-front, but not in the S-front. Numerical diffusion spreads the shock over several zones and structure in the S-front is consequently numerical.

IONIZATION-SHOCK FRONT EVOLUTION

We present results without molecular cooling $\left(\lambda(T) = 0, \text{ Eq. } (1)\right)$. Radiation flux vectors at $t = 4.86 \times 10^9$s (Fig. 2) show absorption at the cloud edge. Flux incident on the cloud face parallel to the bottom boundary is less dilute than that reaching the cloud sides, and more ionization and heating takes place in the former region. This effect is shown in Fig. 3, which plots the ionization energy (in ergs) absorbed during the timestep. The I-front velocity at this time is approximately 6.5 km/s at the cloud's lower face and 4.7 km/s at the side. Cloud geometry, therefore, plays an important role because signals originating at different places along the curved I-front will interact within the cloud.

Ionization at the cloud edge increases both temperature and particle density, enhancing the pressure at the cloud edge. The I-front is initially a weak R-type (Newman and Axford, 1968). As the front penetrates the cloud, the driving flux decreases due to geometric dilution and to absorption by neutral gas moving through the front into the intercloud medium. The I-front velocity falls below that of an R-critical type and a preceding strong shock develops. Due to increased shock compression, the I-front velocity slows and it becomes a D-type. At $t = 6.6 \times 10^9$s, one notes the appearance (Fig. 4) of a strong pressure peak in the S-front, still imbedded in the I-front

This correction is on a correction sheet in the camera ready manuscript.

region at T = 10-13000°K. When the shock reaches 6 km/s velocity at Mach number, M = 15, jump conditions predict $p_2/p_1 = 280$, in reasonable agreement with the numerical value 300.

Velocities of gas particles at $t = 1.8 \times 10^{10}$s in Fig. 5 show bifurcation at the cloud edges where material moves toward the cloud interior or is accelerated into the rarified intercloud medium. Also apparent is the coalescence of flows from the side and the cloud face. This effect of cloud geometry causes a compression of the gas at $r = 8.0 \times 10^{15}$, $z = 2.7 \times 10^{16}$ to values higher than present in other portions of the curved shock. The material blown into the intercloud medium exits the I-front with velocity 1-2 km/s and accelerates to about 20 km/s when it leaves the computing mesh. This agrees with Spitzer's qualitative treatment.

Temperature in the I-front is affected by the balance of ionization heating, recombination cooling, and pdV work. The effects of conduction and viscous heating are small. At $t = 1.8 \times 10^{10}$s, along the symmetry axis, the shock ($p - \rho$ peak) in Fig. 6 completely detaches from the I-front region. Defining subscripts 1 (ahead, X = 0.001) and 2 (behind, X = 0.98) the I-front in the usual convention, we find that $M_1 < 1.0$, $M_2 > 1.0$; $p_1 > p_2$; $\rho_1 > \rho_2$; and $v_2 > v_1$, thus the I-front is a strong D type with average temperature T = 9000°K. The density ratio (ρ_2/ρ_1) in the shock at 1.8×10^{10}s is 3.7, approaching the strong shock limit 4.0. The ratio in the region of flow convergence is even higher, as discussed above.

At later times, the flow field carries the region of interest outside the fixed Eulerian mesh Figure 7 shows the density at $t = 3.6 \times 10^{10}$s before the shock leaves the mesh when the compression ratio near the symmetry axis is 3.7 and that in the torroidal flow convergence region is above 6.5. Solution of Poisson's equation for the gravitational potential shows that the neutral gas in the shock and in the flow convergence region is accelerated toward the CPS layer on the symmetry axis. This layer is pressure bounded below by the I-front and above by the shock and, therefore, one anticipates that if enough mass accumulates and/or the Jeans' criterion is reduced by the velocity field, star formation will occur. Further calculations are required, especially ones including dust, before conclusions can be stated in a less speculative manner.

Recent high resolution observations in ^{12}CO and ^{13}CO of the Rosette molecular cloud complex indicate star formation regions that cannot be explained by supernovae shock transit or by the Elmegreen-Lada mechanism (Blitz and Thaddeus, 1980). These authors suggest (prior to our calculations) that star formation may result from I-S front generated implosion of a cloud clump. These calculations indicate that such an implosion results from the multidimensional nature of the I-S front structure, which is in turn caused by the spatial variations in cloud density. This effect is indeed a potentially new mechanism for O-B star formation, and it could change Elmegreen and Lada's time

scale. In addition, VLBI aperture synthesis observations of OH maser sources (Reid et al., 1980) seem to require fragmentation of cloud edges in front of the I-front. I-S implosions that seed star formation can explain these observations without postulating a more distant shock. Preliminary analysis of results with molecular cooling indicate, as expected, that density compression is larger and evolutionary time scales are longer.

SUMMARY

These calculations for a single 09 source star 8 pc distant from the cloud indicate the following.

- I-S front strength and temperatures are enhanced at cloud faces.
- The weak R-type front becomes a strong D-type in less than 600 years, and a strong shock develops.
- Some cloud disruption occurs and velocities of the blow-off to the intercloud medium are 1-20 km/s.
- Cloud geometry produces flow coalescence that increases density locally. This effect can enhance the star formation process near cloud edges. Density compression of 7 occurs in 1700 years.
- Cloud geometry allows the I-front characterization to vary along curved edges.
- Self gravity accelerates material toward the CPS layer.

REFERENCES

1. Ambartsumian, V. A., 1958, "Theoretical Astrophysics," trans J. B. Sykes, Pergamon Press, London.
2. Blaauw, A., 1964, An. Rev. Astron. Astrophys., 2, pp. 213-246.
3. Blitz, L., and Thaddeus, P., 1980, Astrophys. J., 241, in press.
4. Elmegreen, B. G., and Lada, C. J., 1977, Astrophys. J., 214, pp. 725-741.
5. Hunter, J. A., Jr., 1979, Astrophys. J., 233, pp. 946-949.
6. Lathrop, K. D., and Brinkley, F. W., 1973, "TWOTRAN-II: An Interfaced Exportable Version of the TWOTRAN Code for Two Dimensional Transport," Los Alamos Scientific Laboratory Report LA-4848-MS.
7. Lynds, B. T., 1980, Astron. J., 85, pp. 1046-1052.
8. Newman, R. C., and Axford, W. I., 1968, Astrophys. J., 153, pp. 595-614.
9. Reid, M. J., Haschick, A. D., Burke, B. F., Moran, J. M., Johnston, K. J., and Swenson, G. W. Jr., 1980, Astrophys. J., 239, 89-111.
10. Rivard, W. C., and Torrey, M. D., 1977, "KFIX: A Computer Program for Transient Two-Dimensional Two-Fluid Flow," Los Alamos Scientific Laboratory Report LA-NUREG-6623.
11. Spitzer, Lyman Jr., 1978, "Physical Processes in the Interstellar Medium," John Wiley and Sons, New York.
12. Tenorio-Tagle, G., 1976, Astron. and Astrophys., 53, pp. 411-417.

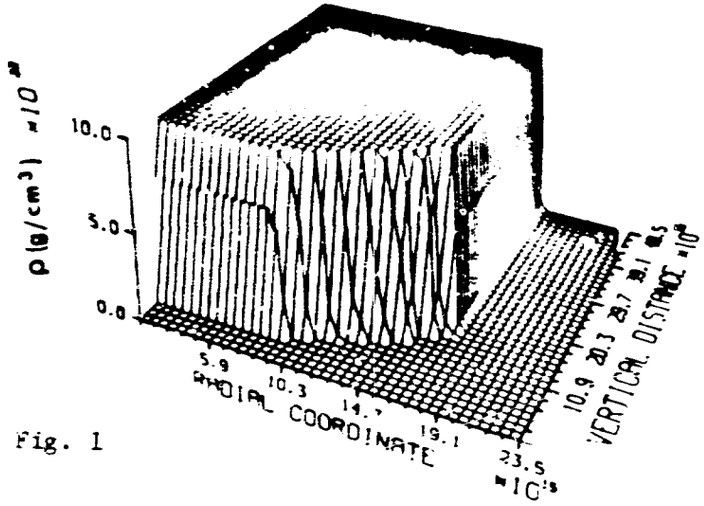

Fig. 1

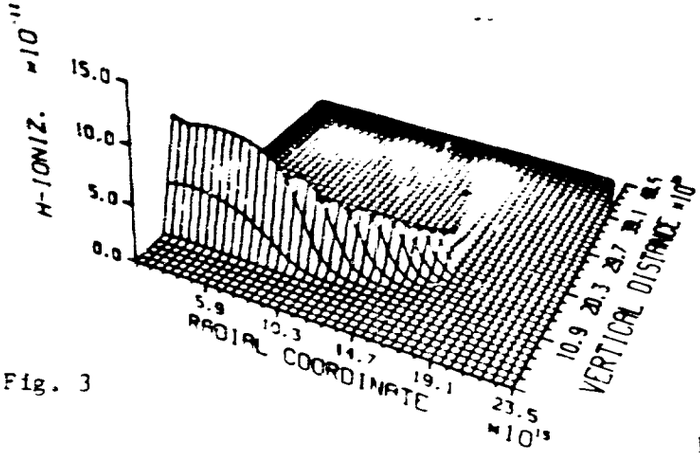

Fig. 3

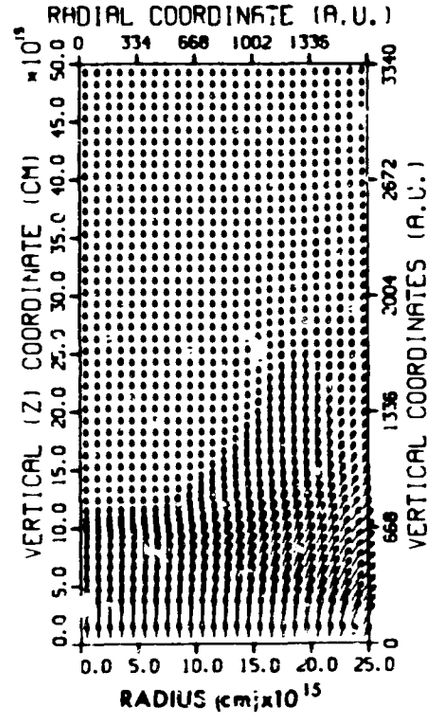

Fig. 2

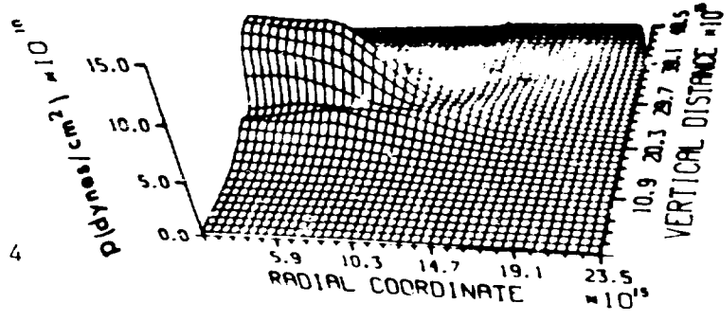

Fig. 4

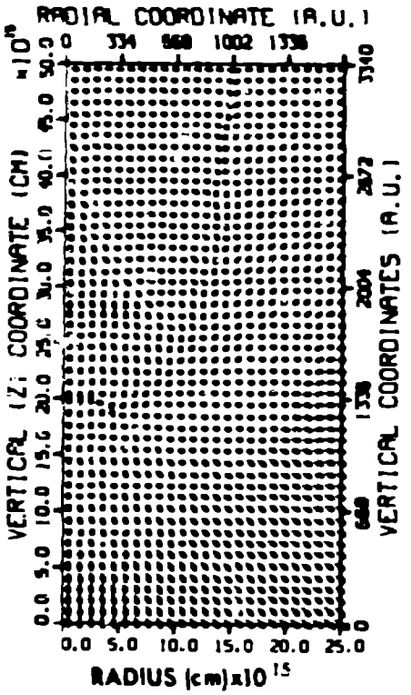

Fig. 5

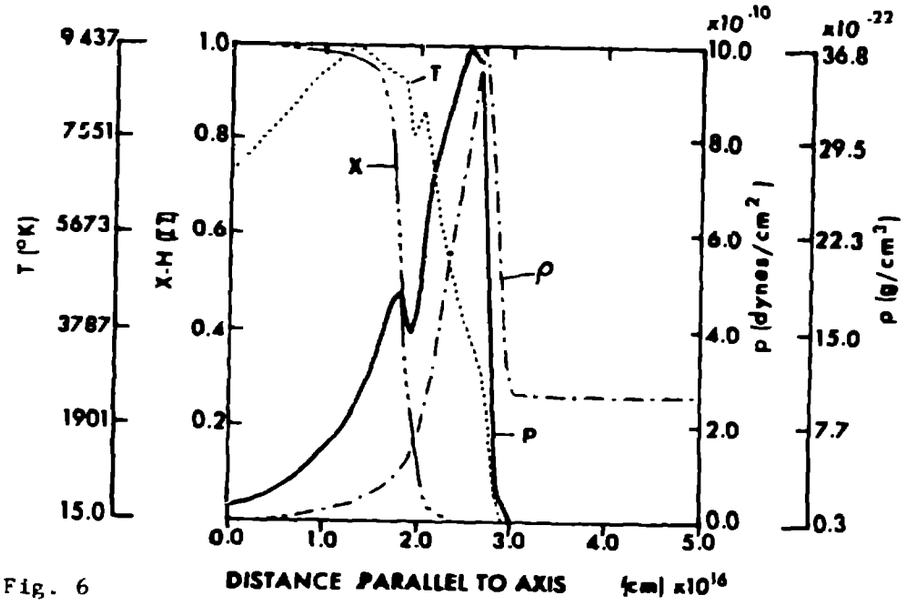

Fig. 6

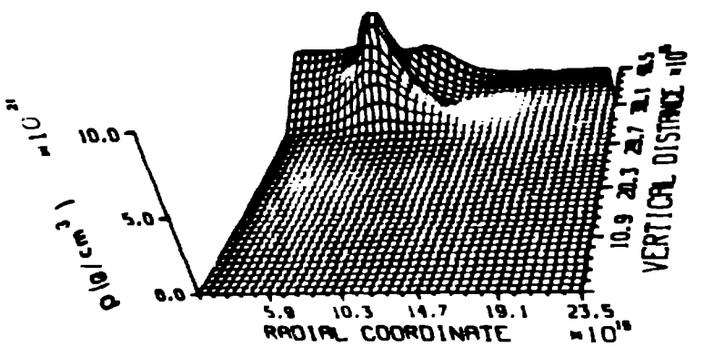

Fig. 7